

# 1

## High-resolution transmission electron microscopy

S. HORIUCHI and L. HE

### 1.1 Introduction

High-resolution transmission electron microscopy (HRTEM) has been widely and effectively used for analyzing crystal structures and lattice imperfections in various kinds of advanced materials on an atomic scale. This is especially the case for high  $T_c$  superconductors (HTSCs). The most characteristic feature in crystal structures of HTSCs is that there is a common structural element, a  $\text{CuO}_2$  plane, in which superconductive carriers (positive holes or electrons) are transported. The remaining part, sandwiching the  $\text{CuO}_2$  planes, accommodates additional oxygen atoms or lattice defects to provide carriers to the  $\text{CuO}_2$  planes. This is known as the charge reservoir. The transition temperature between superconductive and non-superconductive states,  $T_c$ , strongly depends on the concentration of carriers in  $\text{CuO}_2$  planes and the number of  $\text{CuO}_2$  planes. Any charge reservoir is composed of some structural elements, including lattice defects. An aim of HRTEM is to clarify the structure of the charge reservoirs. Additionally, a variety of microstructures strongly affect the critical current density,  $J_c$ , since they closely relate to the weak link at boundaries between superconductive grains as well as to the pinning of magnetic fluxoids. The characterization of point defects, dislocations, stacking faults, precipitates, grain boundaries, interfaces and surface structures is another important aim of HRTEM. In this chapter, we describe some fundamental issues in analyzing crystal structures and microstructures in HTSCs by HRTEM.

### 1.2 Theoretical background for HRTEM

HRTEM images closely depend not only on some optical factors in the imaging process by the electron lens, but also on a scattering process of the electrons

incident on the crystal specimen [1.1]. This section describes the electron-optical background for HRTEM.

### 1.2.1 Phase contrast

Let us begin with a simple case where a central beam and one diffracted beam pass through the objective aperture of an electron microscope. Both beams starting from a site in the bottom surface of a thin specimen meet again at the image plane to form an image. With their contributions at the site  $x_i$  on the image plane,  $\Psi_o(x_i)$  and  $\Psi_g(x_i)$ , the amplitude and intensity of the resultant wave,  $\Psi(x_i)$  and  $I(x_i)$ , can be expressed as

$$\begin{aligned}\Psi(x_i) &= \Psi_o(x_i) + \Psi_g(x_i) \\ I(x_i) &= \Psi(x_i)\Psi^*(x_i) \\ &= I_o(x_i) + I_g(x_i) + 2\text{Re}[\Psi_o(x_i)\Psi_g^*(x_i)],\end{aligned}\quad (1.1)$$

where  $I_o(x_i) = |\Psi_o(x_i)|^2$  and  $I_g(x_i) = |\Psi_g(x_i)|^2$ . Re means that only the real part in the bracket should be considered. Here it is assumed that both waves can interfere coherently.

A phase difference arises between  $\Psi_o(x_i)$  and  $\Psi_g(x_i)$  mainly because of the difference in the path length. As a result, interference fringes (a lattice image) appear in the image. The image contrast is called phase contrast since it owes its origin to the phase difference. For a very thin specimen with an incident beam of unit amplitude,  $I_o = 1 \gg I_g$ ,

$$I(x_i) = 1 + 2\text{Re}[\Psi_g^*(x_i)],\quad (1.2)$$

where the magnification is assumed to be 1. The image contrast is proportional to the diffraction amplitude. This means that appreciable contrast can be obtained even from very small subjects like a single atom, a fine particle or a thin film, whose scattering power is very small. For comparison, the so-called diffraction contrast, another image contrast mechanism widely used for characterizing large scale defects like dislocations, is proportional to the diffracted intensity.

### 1.2.2 Lattice image and structure image

Let us consider the imaging mechanism of a lattice image using Fig. 1.1(a) [1.1]. First, diffraction waves are excited by a substance. After passing through the electron lens the diffraction pattern is formed on the back focal plane. The intensity maximum of each reflection is designated as  $0, \pm 1, \dots, \pm h, \dots$ . Secondly, these spots become new sources so that the electrons starting here



### 1.2.3 Phase contrast transfer function

Electrons change the phase on passing through an electron lens due to the spherical aberration and defocus. The aberration function  $\chi(u)$ , proportional to the change in phase of the electron wave, is described by

$$\chi = \varepsilon\lambda u^2/2 - C_s\lambda^3 u^4/4, \quad (1.4)$$

where  $\varepsilon$  is the amount of defocus,  $\lambda$  the wavelength of electrons,  $u$  the spatial frequency and  $C_s$  the spherical aberration constant [1.2].

The phase factor  $\exp\{2\pi i\chi(u)\}$  in eq. (1.3) strongly affects the intensity of lattice images. The function  $\sin(2\pi\chi)$  is very important to determine, and is called the phase contrast transfer function. Fig. 1.2 shows some calculated results of the function with parameters,  $E$  (accelerating voltage) = 200 kV and  $C_s = 1.2$  mm, for the range between  $\varepsilon = 900$  and  $-500$  Å [1.1]. The horizontal axis is scaled by the value of  $u$  ( $= 1/d$  where  $d$  is the interplanar spacing). The value of the function fluctuates between 1 and  $-1$ . The fluctuation is more prominent at higher ranges of  $u$ . It is noted that  $\sin(2\pi\chi) = 1$  in the range between  $u = 1/2.5$  and  $1/6$  Å<sup>-1</sup> at  $\varepsilon = 650$  Å.

### 1.2.4 Weak phase object approximation

Electrons entering into any material are affected by the electrostatic potential field  $V$  and, as a result, change their phase. For electrons running in the  $z$  direction, the phase change is described by

$$q(r_0) = \exp\left(i\sigma \int V dz\right), \quad (1.5)$$

where  $\sigma$  is the interaction parameter.  $q$  is called the transmission function. When the crystal is so thin that the relation

$$\sigma \int V dz (= \sigma V_p) \ll 1 \quad (1.6)$$

holds, eq. (1.5) can be expanded as follows:

$$q(r_0) = 1 + i\sigma V_p(r_0), \quad (1.7)$$

where  $V_p$  is the projected potential of crystal,  $r_0 = (x_0, y_0)$  the two-dimensional positional vector in the objective plane. This is the approximation of a weak phase object. Since  $i$  represents the phase change of  $\pi/2$ , eq. (1.7) means the sum of the central beam with amplitude 1 and the scattered electron waves with amplitude  $i\sigma V_p(r_0)$ .

On the Fourier transformation of eq. (1.7) we get

$$\mathcal{F}[q(r_0)] = Q(u) = \delta(u) + i\sigma \mathcal{F}[V_p(r_0)] \quad (1.8)$$

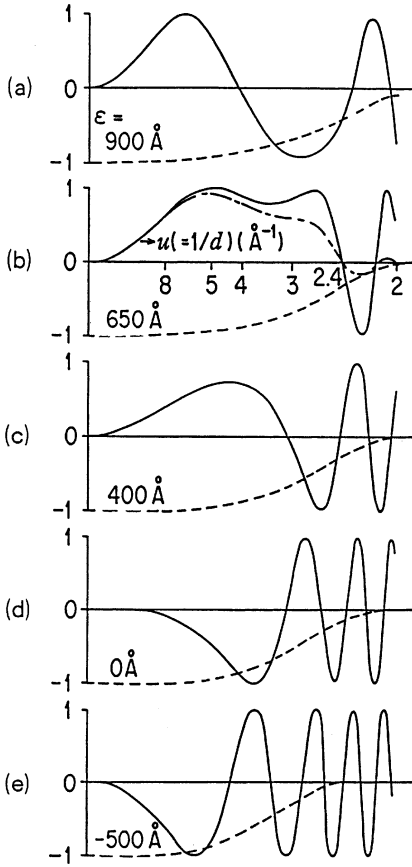


Fig. 1.2. Phase contrast transfer function  $\sin(2\pi\chi)$  (solid line) and attenuation function  $-E_D E_j$  (broken line) against  $u$ , for  $E = 200$  kV and  $C_s = 1.2$  mm.

where  $\delta(u)$  is the delta function. The Fourier transform of the second term has the following value

$$\mathcal{F}[V_p(r_0)] = V_u \Delta z = (48.0/\Omega)F(u)\Delta z, \tag{1.9}$$

where  $V_u$  is the Fourier coefficient of potential,  $\Omega$  the volume of unit-cell and  $F(u)$  the crystal structure factor, the atomic structure factor  $f_j$  summed over sites  $j$ ,

$$F(u) = F_{hk0} + \sum_j f_j \exp[-2\pi i\{h(x_{0j}/a) + k(y_{0j}/b)\}]. \tag{1.10}$$

6 *S. Horiuchi and L. He*

### 1.2.5 Scherzer imaging condition

On substituting eqs. (1.8) and (1.9) into eq. (1.3) we get

$$\begin{aligned}\Psi(r_i) &= \mathcal{F}[\{\delta(u) + i\sigma V_u \Delta z\} \{\cos 2\pi\chi(u) + i \sin 2\pi\chi(u)\}] \\ &= 1 - \sigma \Delta z \mathcal{F}[V_u \{\sin 2\pi\chi(u) - i \cos 2\pi\chi(u)\}]\end{aligned}\quad (1.11)$$

where the size of objective aperture is assumed to be infinite. The image intensity is

$$I(r_i) = 1 - 2\sigma \Delta z \mathcal{F}[V_u \{\sin 2\pi\chi(u)\}]. \quad (1.12)$$

We note from this formula that the image contrast closely depends on the phase contrast transfer function  $\sin 2\pi\chi(u)$ . As shown in Fig. 1.2, the value of  $\sin 2\pi\chi(u)$  changes strongly depending on the defocus  $\varepsilon$ . However, if such a condition as

$$\sin 2\pi\chi(u) = 1 \quad (1.13)$$

holds, the image intensity will be [1.3]

$$I(r_i) = 1 - 2\sigma V_p(r_0). \quad (1.14)$$

Therefore, we can expect that the projected potential  $V_p(r_0)$  is reflected in the image; the site with large value of  $V_p$  shows a dark contrast, while that with low  $V_p$  shows a bright one. This is a general principle for the formation of the structure image; sites of heavy metal atoms having high potential are imaged as dark dots. In order to realize the relation of eq. (1.13) as widely as possible we assume

$$\begin{aligned}2\pi\chi_{\max} &= 0.7\pi \\ \therefore \sin 2\pi\chi_{\max} &= 0.81.\end{aligned}$$

The defocus value corresponding to this,  $\varepsilon_s$ , is

$$\varepsilon_s = 1.2 C_s^{1/2} \lambda^{1/2}. \quad (1.15a)$$

At this defocus the value of spatial frequency,  $u_s$ , for which the value of  $\chi$  first becomes zero, is

$$u_s = 1.5 C_s^{-1/4} \lambda^{-3/4}. \quad (1.15b)$$

Therefore, a structure image can be obtained from a weak phase object first by setting the defocus value at  $\varepsilon_s$  and then by cutting out those diffracted waves whose spatial frequencies are larger than  $u_s$ . These observation conditions derived from eq. (1.13) are called the Scherzer imaging conditions and the defocus value  $\varepsilon_s$  is called the Scherzer focus.

Let us consider the phase change at the Scherzer focus geometrically. In Fig. 1.1(b) solid and broken lines represent the peaks and valleys of the phase, respectively, for the central and diffracted waves [1.1]. For simplicity, only one

diffracted wave is shown. The phase of the diffracted wave is advanced first by  $\pi/2$  on scattering and secondly also by  $\pi/2$  on passing through an electron lens (since  $\sin 2\pi\chi(u) = 1$ ). As a result, the phase difference between the central wave and the diffracted wave becomes  $\pi$ . On the image plane, therefore, destructive interference occurs between them to cause the atom sites to appear dark.

### 1.2.6 Resolution limit for HRTEM

The maximum scattering angle under the Scherzer condition,  $\alpha_{\max}$ , and the corresponding lattice spacing,  $d_s$ , are

$$\alpha_{\max} = \lambda u_s = 1.5 C_s^{-1/4} \lambda^{1/4} \quad (1.16a)$$

$$d_s = 1/u_s = 0.65 C_s^{1/4} \lambda^{3/4} \quad (1.16b)$$

$d_s$  is the minimum spacing in the information contributing to imaging and is called the resolution limit due to spherical aberration, or the Scherzer resolution limit. It is essentially the resolving power of HRTEM. We note from this that  $C_s$  and  $\lambda$  must be made smaller to obtain a higher resolving power.

### 1.2.7 Extension of weak phase object approximation

The weak phase object approximation (eq. (1.6)) is satisfied when  $V_p (= V_0 \Delta z) \ll 1.2 \times 10^3 \text{ V\AA}$  for  $E = 200 \text{ kV}$ . This means  $\Delta z \ll 120 \sim 40 \text{ \AA}$  since  $V_0$  (mean inner potential) =  $10 \sim 30 \text{ V}$  for most inorganic crystals. In reality, however, structure images are obtained mostly for thickness between 15 and 50  $\text{\AA}$ , depending on the material, crystal structure and orientation, and accelerating voltage. That is to say, the condition for the weak phase object is not satisfied in most actual cases.

In order to overcome this contradiction we extend the theory of weak phase object approximation to slightly thicker crystals as follows; from dynamical calculations on the amplitude and phase of many waves we note the existence of such a relation as

$$Q(u) = Q'(u) \exp(iB\Delta z) \quad (1.17)$$

where  $B$  is constant for each of the scattered waves and 0 for the central wave as long as the crystal thickness is less than that for the first extinction. Besides, the amplitude of the scattered waves is still considerably less than that of the central wave, and the relative intensities of the scattered waves are almost the same as for kinematical scattering [1.4]. It is therefore reasonable to assume that  $\mathcal{F}[Q'(u)]$  essentially resembles  $\exp(i\sigma V_p)$ . Then we obtain

8 *S. Horiuchi and L. He*

$$\Psi(r_i) \propto \exp\{i\sigma V_p(r_0)\} * \mathcal{F}[\exp\{2\pi i(\chi + B\Delta z)\}] \quad (1.18)$$

where  $*$  means the convolution integral and the size of the objective aperture is assumed to be infinite. A similar formula can be derived from wave mechanical considerations [1.1]. Eq. (1.18) means that we have only to consider the effect of the total phase change. The wave aberration  $2\pi\chi$  and the phase change  $2\pi B\Delta z$  due to the dynamical effect of electron diffraction are therefore equivalent from the viewpoint of the transfer of phase contrast. The Scherzer imaging condition (eq. (1.13)) should then be modified to

$$\sin\{2\pi(\chi + B\Delta z)\} = 1. \quad (1.19)$$

In fact, the optimum focus at which the structure image is obtained is in most cases not at the Scherzer focus  $\varepsilon_s$  (eq. (15a)) but slightly shifted towards the Gaussian focus, depending on thickness. This is due to the effect of the phase shift by the dynamical scattering. According to a numerical calculation, for example [1.1], the main part of the modified transfer function already deviates from the condition of  $\sin 2\pi\chi = 1$  at a thickness of only 16 Å for a crystal with heavy elements such as  $2\text{Nb}_2\text{O}_5 \cdot 7\text{WO}_3$ , and the optimum defocus shifts from 1000 to 500 Å for a thickness near 50 Å.

### 1.2.8 Effect of the coherence among electron waves

On the formation of lattice images the amplitudes of waves are integrated. This means that we must consider the interference among them under coherent conditions. In fact, the chromatic aberration and the beam convergence effects seriously deteriorate the coherence and, as a result, the image intensity is decreased. The degree of coherence among electron waves can be described by a function which is called the transmission cross coefficient. Using this function we can estimate the effect of the coherence degradation for the weak phase object as follows

$$I(r_i) = 1 - 2\sigma\Delta z \mathcal{F}[V_u \sin\{2\pi\chi(u)\} E_D(u, \varepsilon) E_j(u, \varepsilon)] \quad (1.20a)$$

$$E_D(u, \varepsilon) = \exp(-0.5\pi^2\lambda^2\Delta^2 u^4) \quad (1.20b)$$

$$E_j(u, \varepsilon) = \exp\{-(\pi u_0)^2[(\varepsilon - C_s\lambda^2 u^2)\lambda u]^2\} \quad (1.20c)$$

where  $\Delta$  is the mean fluctuation of focus due to the chromatic aberration and  $u_0$  the effective size of the electron source ( $u_0 = \beta/\lambda$ , where  $\beta$  is the semi-angle of the illumination convergence). On comparing with eq. (1.12) we note that the phase contrast transfer function  $\sin\{2\pi\chi(u)\}$  is attenuated by the modulation function  $E_j(u, \varepsilon)E_D(u, \varepsilon)$ . In Fig. 1.2 the values of  $-E_jE_D$  are plotted by broken lines. An example of the effective transfer function, obtained by the product between this and  $\sin\{2\pi\chi(u)\}$ , is shown by a chain line in Fig.

1.2(b). In the region of large spatial frequency the attenuation of the transfer function is prominent.

### 1.3 Techniques relevant to HRTEM

#### 1.3.1 *Electron-optical conditions to obtain an HRTEM image*

Many-beam lattice images are usually obtained under the following electron-optical conditions. (1) The illuminating electron beam is axial. (2) It is incident along a low-order zone axis of the crystal. (3) The objective aperture has the size given by eq. (1.15b) or (1.16). (4) The specimen crystal is very thin. (5) The image is observed at the defocus given by eq. (1.15a), or, it is slightly shifted toward the Gaussian focus, depending on the thickness, as mentioned in relation to eq. (1.19).

A structure image appears in a through-focal series of many-beam lattice images. For getting a structure image, the specimen thickness must be thinner than a few tens of ångströms. Except for the case when a specimen is originally prepared as a thin film, this is achieved only by crushing a bulk material. The crushing method is applicable to crystals which break into fragments by cleavage.

On the other hand, for the observation of cross-sections of materials, for example prepared by CVD methods, specimens must be thinned by an ion-milling method. The resulting thickness is generally more than 100 Å. This means an optical artifact inevitably arises in the image, i.e. the correspondence between the image contrast and the crystal structure is no longer unique. The interpretation of such an image must be done even more carefully, using computer simulations of image intensities.

#### 1.3.2 *Procedure for observing an HRTEM image*

A practical procedure for observing a many-beam lattice image is as follows. For simplicity, we assume a specimen fragment in the form of a sharp wedge is used, which has been prepared by the crushing method and supported on a carbon microgrid. (1) The specimen is observed with a magnification of about  $1 \times 10^4$  times to look for an area which is very thin, clean and not distorted, at the edge of a fragment. (2) The orientation of a small crystal area is examined by means of a diffraction pattern. When Laue zones are found suggesting that the orientation is near to that intended, the tilting stage is operated so that the zone axis becomes parallel to the optical axis. (3) An objective aperture is inserted at the center of the diffraction pattern. (4) After confirmation of

voltage center, astigmatism is corrected by use of a stigmator. This is done by observing the granular structure of a microgrid film enlarged on a TV screen. (5) On changing slowly the amount of defocus, photographs are taken when the images anticipated in advance by means of the computer simulation of image intensity appear. For an unknown structure an image with high contrast appearing nearly at the Scherzer focus is recorded, and then several images are taken changing the defocus value for each in the direction to the Gaussian focus (a through-focal series of images). (6) A diffraction pattern is recorded to check how far the orientation has deviated from the zone axis during this procedure.

### ***1.3.3 Computer simulation of an HRTEM image***

Whether a structure model of a crystal or a defect obtained from an HRTEM image is correct or not must be examined. The method most widely practiced at present is to compare experimental images to calculated images obtained by computer simulation based on the structure model. The image intensity can be computed using commercially available or home-made software [1.1]. The calculation consists of two stages, i.e. the scattering stage and the imaging stage. In the former, dynamical diffraction amplitudes are computed usually by the multi-slice method [1.5]. During the course of this stage the projected potential of the crystal is also calculated.

### ***1.3.4 Use of information from electron diffraction***

Electron diffraction patterns include a great deal of information on crystal structure. They give valuable information that is complementary to that obtained from HTREM images, because they give more average and statistically significant information than images. For an example, lattice parameters are obtained more precisely from diffraction patterns than from images. Another example is the crystal symmetry and the related space group, which is derived from the extinctions of diffraction spots [1.1]. These are demonstrated by some concrete examples later.

## **1.4 HRTEM analysis of high $T_c$ superconductors**

In this section, some recent results on the structure analysis of HTSCs are shown in order to demonstrate the usefulness of HRTEM. In all cases mentioned here small blocks of specimens were lightly crushed in an agate mortar and the fragments obtained were observed in a high-resolution, high-voltage